

Particle reacceleration in the Coma cluster and the radio, EUV and hard X-ray emissions.

G. Brunetti^{1,2}, L. Feretti², G. Giovannini^{3,2}, and G. Setti^{1,2}

¹ Dip. di Astronomia, Univ. di Bologna, via Ranzani 1, I-40127 Bologna, Italy

² Istituto di Radioastronomia del CNR, via Gobetti 101, I-40129 Bologna, Italy

³ Dip. di Fisica, Univ. di Bologna, via Berti-Pichat 6/2, I-40127 Bologna, Italy

Abstract. The radio spectral index map of the Coma halo shows a progressive steepening of the spectral index with increasing radius. Such a steepening cannot be simply justified by models involving continuous injection of fresh particles in the Coma halo or by models involving diffusion of fresh electrons from the central regions.

We propose a scenario in which the relativistic particles injected in the Coma cluster by some processes (merger, accretion shocks, turbulence) are systematically reaccelerated for a relatively long time (~ 1 Gyr). We show that such a scenario can account for the synchrotron radio spectral index distribution, for the radio halo size at different frequencies, and for the total (integrated) radio spectrum of the Coma halo. We also show that for a suitable choice of the parameters the model can also account for the hard X-ray flux observed by BeppoSAX via the inverse Compton scattering of the cosmic microwave background radiation by the synchrotron electrons. The possibility to account for the EUV flux detected with the EUVE satellite by the inverse Compton emission is also discussed.

1. Introduction

The Coma halo is the most famous example of a diffuse radio emission in clusters of galaxies.

At the lowest frequencies the radio emission extends up to $\sim 30 - 40$ arcmin from the center (e.g. Hanisch & Erickson 1980 at 43 MHz; Henning 1989 at 30.9 MHz), while at higher frequencies detailed radio images have been obtained at 327 MHz (Venturi et al. 1990) and at 1.38 GHz (Kim et al. 1990). By applying Gaussian fits it has been found that the 327 MHz FWHM (28×20 arcmin) is significantly larger than that inferred at 1.38 GHz (18.7×13.7 arcmin), but smaller than the low frequency size.

The 327–1400 MHz spectral index map of the Coma halo shows that the spectrum steepens rapidly with increasing distance from the center (Giovannini et al. 1993).

The Coma halo has also been observed with the Effelsberg single-dish 100 m telescope (Deiss et al. 1997, at 1.4 GHz; Schlickeiser et al. 1987, at 2.7 GHz). The 1.4 GHz observations reveal a flux density at large scales higher

than that measured with the synthesis aperture instruments and confirm a spectral index steepening with increasing radius. The 2.7 GHz measurements appear to be inconsistent with these results suggesting that the Schlickeiser et al. integrated flux may be underestimated (Deiss et al. 1997).

Lieu et al. (1996) have detected extreme ultraviolet emission (EUV) in excess to that expected by extrapolating downward the thermal X-ray spectrum emitted by the intracluster gas ($kT = 8.21$ keV). Recently, Fusco-Femiano et al. (1999) have discovered an hard X-ray tail exceeding the thermal emission.

Synchrotron emission in the radio band, inverse Compton (IC) emission in the EUV and hard X-rays from cluster of galaxies are expected in the framework of continuous injection of primary relativistic electrons (Sarazin 1999; Völk & Atoyan 1999). The models invoking a secondary production of the relativistic electrons also predict a large gamma-ray flux from neutral pion decay; in the case of Coma, an IC origin of the hard X-ray tail would lead to a gamma-ray flux considerably larger than the EGRET upper limit (Blasi & Colafrancesco 1999).

In this paper we will assume $H_0 = 75 \text{ km s}^{-1} \text{ Mpc}^{-1}$.

2. A model with systematic reacceleration

2.1. The spectral steepening problem

A model should be able to reproduce the observed steepening in the radio spectral index distribution, the integrated radio spectrum and the brightness distribution observed at different frequencies.

The spectral steepening with radius is probably the most difficult to reproduce. It cannot be related to the diffusion of fast ageing particles from the central part into the cluster volume, because the diffusion velocity is relatively low (Berezinsky et al. 1997) and the diffusion time is too large compared to the radiative time of the relativistic electrons (Sarazin 1999).

Alternatively one might consider a continuous injection of fresh particles in the cluster volume. To justify the steep spectrum observed in the peripheral regions of the

Coma cluster one would have to assume a space modulation of the injection rate such that the injection is progressively stopped moving from the periphery toward the center in a crossing time smaller than the radiative time of the emitting particles. This appears to be difficult to achieve in the Coma cluster, since the physical mechanism responsible for such a modulation should then propagate at a velocity 20–50 times larger than the sound speed.

It may be thought that these problems can be solved by assuming that the spectrum of the continuously injected particles is steeper with increasing distance from the cluster center. However, it can be shown that the superposition of the corresponding synchrotron spectra, constrained by the observed brightness distribution, leads to an integral spectrum flat at high frequencies ($\sim 0.6 - 0.7$) and steep at low frequencies ($\sim 1.4 - 1.7$), in contrast with the observations that do not show a substantial flattening of the spectrum at high frequencies.

2.2. The effect of systematic reacceleration on the particle spectrum

In order to avoid the above mentioned difficulties, we investigate the possibility that systematic reacceleration is present in the cluster gas and propose a two phases scenario for the Coma halo.

During the first phase the particles are injected and reaccelerated over the cluster volume (starting at t_2) for a relatively long time ($t_1 - t_2 \sim 1-3$ Gyrs) by a major merger event; evidence of a recent merging has been pointed out (see Briel et al. 1992 for a discussion on recent mergings). We further assume that following the injection phase the particles are being systematically reaccelerated for a relatively short time ($\tau \equiv t_0 - t_1$) till the present cosmic time t_0 by secondary accretion shocks and/or turbulence.

By assuming a power law injection spectrum ($\propto q\gamma^{-\text{delta}}$), the evolution of the particle density during the injection phase can be obtained by solving the kinetic equation (Kardashev 1962):

$$\frac{\partial N(\gamma, t)}{\partial t} = \frac{\partial}{\partial \gamma}[-2\beta\gamma + \alpha] + q\gamma^{-\delta} \quad (1)$$

with β the radiative losses ($d\gamma/dt = -\beta\gamma^2$) and $\alpha \sim 1/T_a$ the rate of systematic reacceleration.

We assume that the main cooling mechanism for the relativistic particles in the Coma cluster is the IC scattering with the CMB photons, implying an average strength of the magnetic field $B \leq 3\mu\text{G}$ across the cluster.

The solution for the first phase, at time $t_1 - t_2$, is given by:

$$N(\gamma, t_2, t_1) = \frac{q}{\alpha(\delta - 1)} \gamma^{-\delta} \frac{1 - e^{-\alpha(t_1 - t_2)}}{\left[1 - \frac{\gamma}{\gamma_b^0} - e^{-\alpha(t_1 - t_2)}\right]} \cdot \left\{e^{(\delta-1)\alpha(t_1 - t_2)} \left[1 - \frac{\gamma}{\gamma_b^0}\right]^{\delta-1} - 1\right\} \quad (2)$$

for $\gamma \leq \gamma_b^0 \equiv \alpha/\{\beta(1 - e^{-\alpha(t_1 - t_2)})\}$, and

$$N(\gamma, t_2, t_1) = \frac{q\gamma^{-\delta}(1 - e^{-\alpha(t_1 - t_2)})}{\alpha(\delta - 1)} \left[\frac{\gamma}{\gamma_b^0} + e^{-\alpha(t_1 - t_2)} - 1\right]^{-1} \quad (3)$$

for $\gamma > \gamma_b^0$.

If the particles are reaccelerated during the second phase for a time $\tau = t_0 - t_1$, from Eq.(2) (under our assumptions the majority of the particles follow Eq.2) the spectrum becomes:

$$N(\gamma, \tau, t_2, t_1) = \frac{qe^{\alpha\tau(\delta-1)}}{\alpha(\delta - 1)} (1 - e^{-\alpha(t_1 - t_2)}) \gamma^{-\delta} \left(1 - \frac{\gamma}{\gamma_b}\right)^{\delta-2} \cdot \left\{1 - e^{-\alpha(t_1 - t_2)} - \frac{\gamma}{\gamma_b^0} e^{-\alpha\tau} \left(1 - \frac{\gamma}{\gamma_b}\right)^{-1}\right\}^{-1} \cdot \left\{e^{(\delta-1)\alpha(t_1 - t_2)} \left[1 - \frac{\gamma e^{-\alpha\tau}}{\left(1 - \frac{\gamma}{\gamma_b}\right)\gamma_b^0}\right]^{\delta-1} - 1\right\} \quad (4)$$

for $\gamma \leq \gamma_b \equiv \alpha/\{\beta(1 - e^{-\alpha\tau})\}$, being zero at higher energies.

If the reacceleration is sufficiently efficient, i.e. $\tau \gg 1/\alpha$, Eq.(4) approaches to:¹

$$N(\gamma, \tau) \rightarrow K\gamma^{-\delta} \left(1 - \frac{\gamma}{\gamma_b}\right)^{\delta-2} \quad (5)$$

We remark that, if the second phase is sufficiently long, the reacceleration during the first phase is not necessary to obtain the final shape.

Under the assumption that the electron momenta are isotropically distributed and Eq.(5), the synchrotron emissivity is given by (Jaffe & Perola, 1973):

$$j\left(\frac{\nu}{\nu_b}\right) = \sqrt{3} \frac{e^3}{mc^2} KB\gamma_b^{1-\delta} \int_0^{\pi/2} d\theta \sin^2\theta \cdot \int_0^1 dx F\left(\frac{\nu/\nu_b}{x^2 \sin\theta}\right) x^{-\delta} (1-x)^{\delta-2} \quad (6)$$

where θ is the pitch angle, and ν_b is the critical frequency ($\theta = 90^\circ$, $\gamma = \gamma_b$).

2.3. Modeling the Coma halo

Deiss et al.(1997) derived relationships between the observed spectral index and the intrinsic spectral index distribution of the synchrotron emission assuming a spherical symmetry of the relevant physical quantities. By assuming a Gaussian spatial profile of the emission coefficient they derive the intrinsic spectral index at a given radius and

¹ It should be noticed that Eq.(5) holds for an initial power law energy spectrum $f(\gamma) \propto p^{-\delta}$ without low energy cut-off. In the case of a low energy cut-off and/or Coulomb losses the evolution of the particle energy distribution is much more complicated (Brunetti et al. 1999), but the main results of the model are still valid.

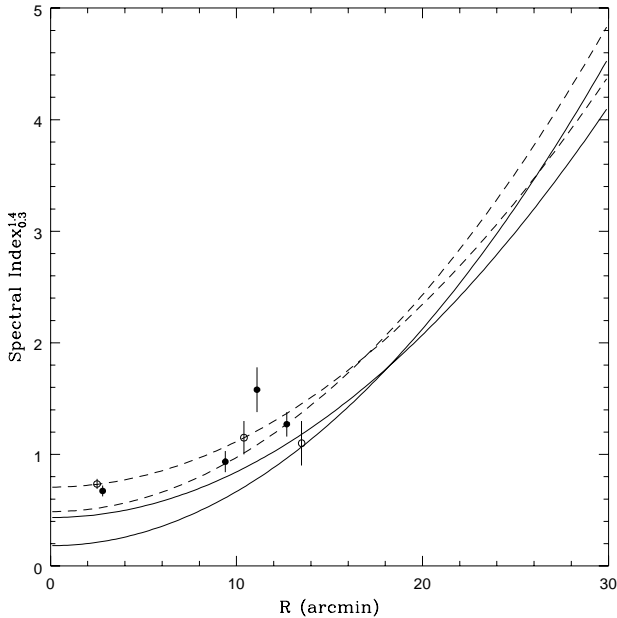


Fig. 1. The predicted observable (dashed lines) and intrinsic (solid lines) spectral index for the Coma halo are reported as a function of the distance from the center. The curves are obtained from Deiss et al.(1997) relationships based on 327/1380 MHz (bottom dashed/solid lines on left corner) and on 327 (single dish)/ 1400 MHz observations. The points are taken from two slices (open and filled circles respectively) through the spectral index map (327–1380 MHz) of Giovannini et al.(1993).

the observed spectral index at the same radius (projected on the plane of the sky) as a function of observable quantities. In the case of the Coma halo they have shown that the FWHMs and flux densities of the radio observations (Venturi et al. 1990; Kim et al. 1990) can be reproduced by a central intrinsic spectral index ~ 0.4 , leading to a central observed spectral index of $\sim 0.6 - 0.8$, in agreement with Giovannini et al. (1993) findings. In Fig.1 we plot the observed and intrinsic spectral index predicted for the Coma halo from Deiss et al. (1997) relationships based on the measurements at 327 MHz (Venturi et al.1990), 1.38 GHz (Kim et al. 1990), and 1.4 GHz (Deiss et al. 1997). The points in Fig. 1 are taken from two different slices through the Coma halo (Giovannini et al. 1993).

From Eq.(6) we obtain the shape of the synchrotron spectrum as a function of the frequency measured in terms of the break frequency ν_b . By calculating the spectral index between two nominal frequencies of constant ratio 1.4 GHz/327MHz, the break frequency $\nu_b(R) \propto B(R)\gamma_b^2(R)$ is obtained when the calculated matches the intrinsic spectral index of Fig.1. The break frequency as a function of R is represented in Fig.2 for several values of the injected electron spectral index δ . Due to the very flat intrinsic spectral index at the center of the Coma halo ($\alpha_{0.3}^{1.4} \sim 0.4$),

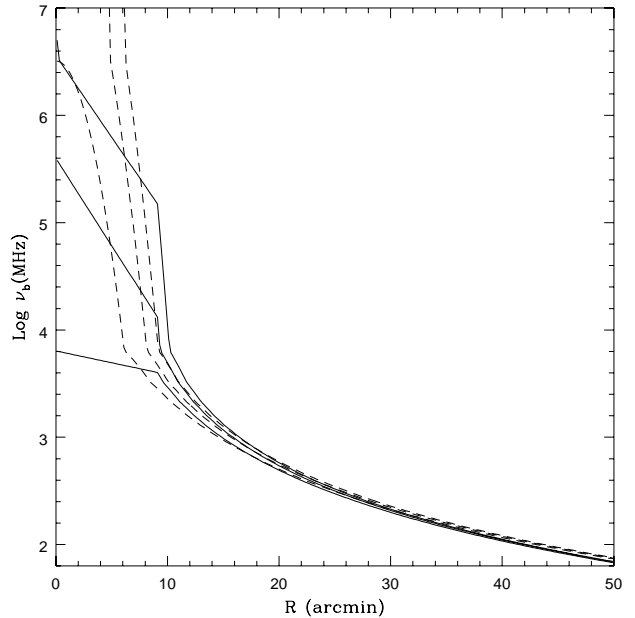


Fig. 2. The calculated intrinsic break frequency is given as a function of the distance R from the cluster center. The calculations are performed by assuming the 327–1380 MHz intrinsic spectral indices (dashed lines) as shown in Fig.1, or the mean spectral index between 327/1380 MHz and 327/(single dish) 1400 MHz measurements (solid lines; here a correction for non-spherical symmetry has been applied to the Deiss et al.(1997) relationships). The values are reported for three different δ : 1.84, 2.01, 2.12 respectively from the bottom of the diagram.

the models with $\delta \geq 1.8 - 1.9$ cannot match the data within ~ 10 arcmin from the center and the break frequency goes to infinity (Fig.2). A correction to Deiss et al. (1997) relationships, due to the non perfect spherical symmetry of the Coma halo (we assume it elongated on the plane of the sky), produces a steeper intrinsic radio spectral indices in the central part of the cluster allowing also the models with $\delta \sim 2$ to converge. However, since we do not know the three-dimensional structure of the Coma halo, the modeling of the central ~ 10 arcmin and the determination of the physical properties remain uncertain.

As a zero order approximation we assume that the large scale magnetic field B is approximately constant over the volume of the cluster. In this case, different break frequencies in the synchrotron spectrum directly correspond to different break energies in the electron energy distribution, i.e. different reacceleration times (α^{-1} , $\gamma_b \rightarrow \alpha/\beta$). In Fig.3 we give the reacceleration time as a function of R for a number of choices of the intracluster magnetic field. In order to explain the very flat intrinsic radio spectrum in the cluster center the efficiency of the reacceleration should rapidly increase and the reacceleration time should become smaller toward the central region, whereas in the

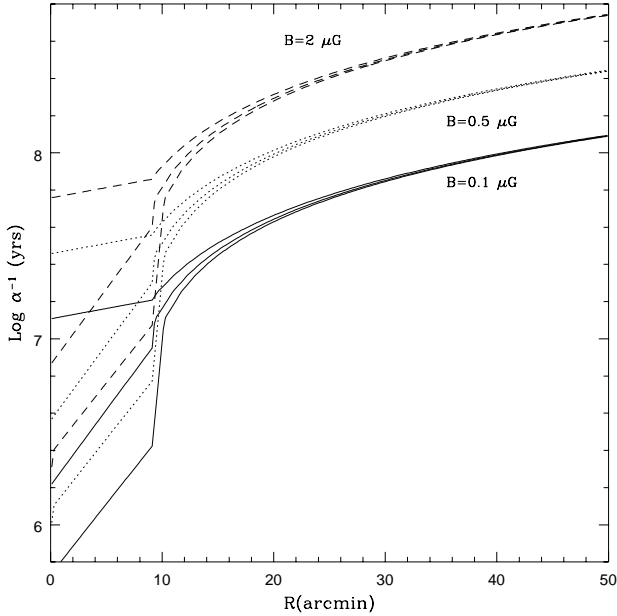


Fig. 3. The reacceleration time is given as a function of the distance R from the center. The calculations are reported for different magnetic field strengths: $0.1 \mu\text{G}$ (solid lines), $0.5 \mu\text{G}$ (dotted lines), and $2 \mu\text{G}$ (dashed lines). From each value of B , we plot three curves corresponding to $\delta=1.84$, 2.01 , and 2.12 starting from the bottom of the diagram. As in Fig.2 a correction for the non spherical symmetry of the Coma halo has been applied.

peripheral regions the reacceleration times are larger than $\sim 3 \cdot 10^7$ yrs. By integrating Eq.(6) along the line of sight we obtain the radio brightness at a given frequency as a function of the projected distance from the center. Given the magnetic field strength B and the geometry, the brightness is a function of the normalization $K(R)$ of the emitting electron population. The model should reproduce the FWHMs of the radio brightness observed at different frequencies (327 MHz, 1380 MHz, and 1400 MHz); by comparing the predicted and observed FWHMs one obtains $K(R)$. We find that a good representation is a β -model-type function : $K(R) = K_0 \{1 + (R(\text{arcmin})/17.5)^2\}^{-1.5}$, where K_0 depends on the assumed value of B .

The model at this point can reproduce both the observed and intrinsic synchrotron spectral indices between 327 and 1400 MHz and the observed FWHMs of the brightness distribution at these frequencies. A fundamental test is to check whether the model can reproduce the shape of the total synchrotron spectrum observed from the Coma halo. We have then integrated Eq.(6), with the derived $\nu_b(R)$ (Fig.2, solid lines) and $K(R)$, over the volume. The result is given in Fig.4 for the representative value $\delta = 2.12$ (the results with δ between 1.9–2.2 being very similar); the model appears to be well consistent with the data.

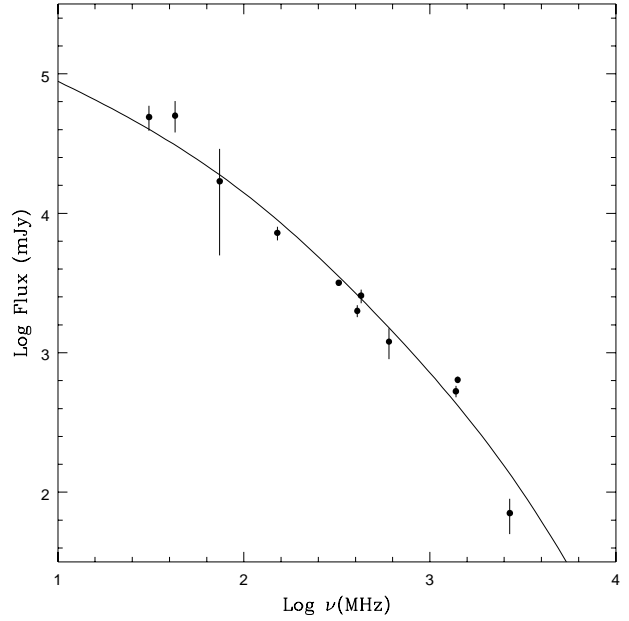


Fig. 4. The calculated total radio spectrum of the Coma halo is compared with the observed fluxes. The calculation is performed by assuming $\delta = 2.12$ (see the text). The data are taken from Table 1 of Deiss et al.(1997).

3. Hard X-rays and EUV emission

3.1. The hard X-ray tail and EUV in the Coma cluster

From a deep BeppoSAX observation, Fusco-Femiano et al.(1999) discovered an hard X-ray tail in the range 20–80 keV exceeding the extrapolation of the thermal X-ray emission spectrum; this excess has also been confirmed by an RXTE observation (Rephaeli et al. 1999). Due to the poor statistics, the spectrum is not well constrained and the origin of this high energy emission cannot be firmly established. It can be generated in non-thermal processes, possibly IC of the radio emitting electrons with the CMB photons (Fusco-Femiano et al. 1999; Sarazin et al. 1999; Sarazin & Lieu 1998), or it might originate from a supra-thermal power law tail of particles emitting via relativistic bremsstrahlung (Ensslin et al. 1999). Furthermore, as recently shown in detail (Dogiel, these proceedings), it could also be of thermal origin (from a modification of the pure maxwellian distribution of the hot cluster gas induced by strong acceleration processes).

The IC origin is particularly fascinating in view of the fact that a comparison between the radio emission from the halo and the hard X-ray tail discovered by BeppoSAX allows to calculate the average strength (over the cluster volume) of the magnetic field B (Fusco-Femiano et al. 1999).

Since in the present model the break energy of the electron population depends on the distance from the cluster center, the synchrotron as well as the IC spectra are

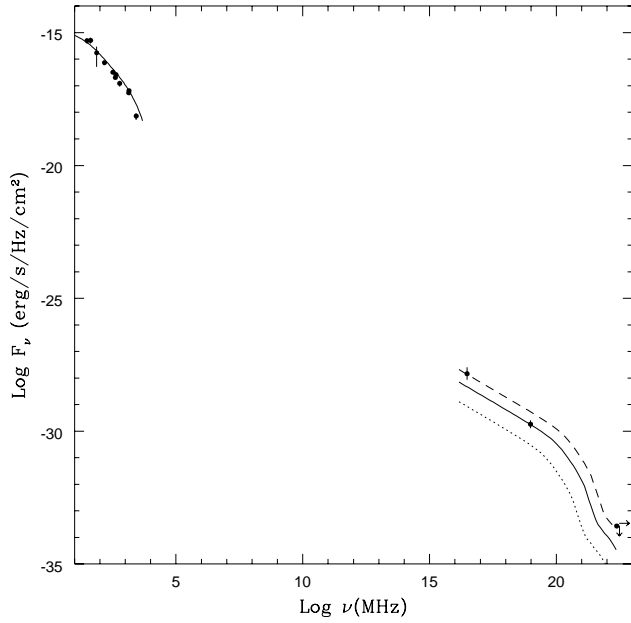


Fig. 5. The expected radio and X-ray IC fluxes are shown and compared with the radio (from Deiss et al.1997), EUV (Bowyer & Berghöfer 1998; Ensslin et al. 1999), hard X-ray (Fusco-Femiano 1999), and gamma-ray (Sreekumar et al. 1996) data. The calculation of the IC flux ($\delta = 2.12$) is shown for different magnetic field strengths: $0.5\mu G$ (dotted line), $0.1\mu G$ (solid line), and $0.05\mu G$ (dashed line).

emitted by relativistic electrons whose energy distribution cannot be represented by a unique power law over all the volume. Therefore, the magnetic field cannot be simply evaluated by standard formulae (e.g. Harris & Grindlay 1979). Under our assumptions the IC emissivity per unit energy and solid angle in the Thomson approximation is given by:

$$j(\epsilon_1) = K(R) \frac{r_0^2 \pi \epsilon_1}{8c^2 h^3} \int \frac{d\epsilon}{e^{\epsilon/kT_{CMB}} - 1} \int_{\gamma_{min}}^{\gamma_b(R)} \frac{d\gamma}{\gamma^{\delta+4}} \left(1 - \frac{\gamma}{\gamma_b(R)}\right)^{\delta-2} \left(2\epsilon_1 \ln \frac{\epsilon_1}{4\gamma^2 \epsilon} + \epsilon_1 + 4\gamma^2 \epsilon - \frac{\epsilon_1^2}{2\gamma^2 \epsilon}\right) \quad (7)$$

where ϵ is the energy of the CMB photons and for ultra-relativistic electrons $\gamma_{min} = \sqrt{\epsilon_1/4\epsilon}$ (e.g. Blumenthal & Gould 1970). The total IC emission is readily obtained by integrating Eq.(7) over the volume.

In Fig.5 we plot the expected IC flux from our model for different magnetic fields and compare the results with the observations; the calculations are performed for $\delta = 2.12$ (in the model the value of B is stable with $\delta \sim 1.9 - 2.2$). Clearly the model cannot account at the same time for the observed EUVs, X-rays and gamma-ray upper limits. The X-ray data are well accounted for by a magnetic field $B \sim 0.1\mu G$, in agreement with the strength

of a large scale magnetic field requested by Faraday rotation measurements (Feretti et al. 1995). Furthermore, it should be noticed that the effect due to Coulomb losses on the electron energy distribution has not been taken into account in the IC calculation of Fig.5. These losses depress the electron energy distribution at low energies ($\gamma < 300$) so that the estimated IC emission in the EUV band should be considered as an upper limit (the predicted EUV flux would be $\sim 3 - 5$ times smaller than the observed value).

Due to the decrease of the synchrotron break frequency with R , in our model the observed radio FWHMs are expected to be smaller than the predicted IC EUV FWHM. This is contrary to the observational evidence (Bowyer & Berghoefer 1998; Ensslin et al. 1999), but consistent with our IC model which underproduces by a large factor the observed EUV flux.

3.2. An additional electron population ?

If the EUV excess is of non-thermal nature, an additional electron population is requested (Bowyer & Berghoefer 1998; Ensslin et al. 1999). It seems natural to assume an additional population of relativistic electrons, with a relatively steep energy distribution ($\delta \simeq 2.8$), injected in the core of the Coma cluster by Active Galactic Nuclei (AGN).

Since the physical conditions at each radius are the same for the two populations, the break energies of this additional population should be distributed as those of the synchrotron electrons (Fig.2, solid lines). The normalization of the particle spectrum is obtained by imposing that it gives the observed EUV emission via IC scattering with the CMB photons. The radio spectral indices, radio brightness profiles, total synchrotron spectrum and hard X-ray IC emission predicted by our model are not substantially modified by the introduction of this additional electron population due to the assumed steep spectral index.

4. Conclusions

We have studied the effect of a systematic reacceleration on the relativistic plasma in the Coma halo. Systematic reacceleration may compensate for the radiative losses providing a suitable mechanism to solve the problem of the very short radiative life-times of the relativistic electrons in the clusters.

We propose a two phase scenario in which the particles are injected and reaccelerated in the cluster volume for a sufficiently long time ($\sim 1 - 3$ Gyrs), after which they are reaccelerated up to the present time. The first phase (the injection phase) is probably related to a major merger process in which relic particles (cosmic rays from galaxies and/or thermal particles) are (re)accelerated by shocks and/or induced strong turbulence. During the second phase (post major merger phase) the electrons lose energy by emitting radiation and, at the same time, are

reaccelerated by the cluster weather (i.e. galactic winds, accretion shocks, and/or turbulence). The combination of losses and reacceleration produces flat synchrotron spectra in the central region and very steep spectra in the peripheral region well matching the observed radio spectral distribution in the Coma halo. By assuming a constant value of B , the requested reacceleration times are relatively large on the majority of the radio halo volume and the reacceleration can be easily provided by systematic Fermi mechanisms. Strong reaccelerations are requested only in the central region of the Coma halo (especially in the case of a small B which is required by the IC production of the observed hard X-ray tail). The problem of short acceleration times can be eased by assuming a gradual increase of the magnetic field strength toward the center of the cluster. Since this would be necessary only in a small fraction of the cluster volume, our assumption of a constant magnetic field strength over the cluster seems very reasonable.

We show that the model can well reproduce the observed brightness profiles at 327, 1380, and 1400 MHz, and the observed integrated synchrotron spectrum. We have also shown that the model can account for the hard X-ray flux observed with BeppoSAX via the IC scattering of the CMB photons with the synchrotron electrons if a magnetic field $B \sim 0.1 \mu G$ is assumed throughout the cluster medium. In this case, the predicted hard X-ray spectral index is ~ 0.6 and the FWHM of the hard X-ray profile is expected to be $\sim 30 - 35$ arcmin, i.e. considerably larger than the synchrotron FWHM at 327 MHz; obviously, it would be very interesting to test these findings with future observations. The energy of the relativistic electrons reservoir would be $\sim 5 \cdot 10^{60} \text{erg s}^{-1}$, i.e. $\sim 5\%$ of the thermal energy of the intracluster gas, far greater than the energy in the magnetic field.

The EUV excess from the Coma cluster cannot be accounted for by IC scattering of the synchrotron electrons with the CMB photons, the predicted emissivity being a factor 3 – 5 smaller than observed. If the EUV excess is non-thermal, then the presence of an additional population of relativistic particles with a more peaked radial distribution must be assumed. We find that the synchrotron and IC hard X-ray contributions from an additional population of relativistic electrons with a steep spectral index ($\delta = 2.8$), matching the EUV excess via IC scattering with the CMB photons, do not substantially alter the fluxes estimated from the first population. The additional population has a total energy in electrons similar to the first one and may have been injected by AGNs activity within the cluster core during most of the cluster life.

A much more detailed discussion about the time evolution of the relativistic plasma and the emitted synchrotron and IC spectra, including the combined effects of Coulomb losses, systematic reacceleration and magnetic field dependence on R , will be presented in a forthcoming paper (Brunetti et al. 1999).

Acknowledgements. We are grateful to A.Atoyan, S.Colafrancesco, R.Ekers, T.Ensslin for useful discussions during the Ringberg workshop. This work was partly supported by the Italian Ministry for University and Research (MURST) under grant Cofin98-02-32, and by the Italian Space Agency (ASI).

References

- Berezinsky V.S., Blasi P., Ptuskin V.S., 1997, ApJ 487, 529
 Blasi P., Colafrancesco S., 1999, *Astropart. Physics* in press; astro-ph/9905122
 Blumenthal G.R., Gould R.J., 1970 *Rev. of Mod. Phys.* 42, 237
 Bowyer S., Berghöfer T.W., 1998, ApJ 506, 502
 Briel U.G., Henry J.P., Böhringer H., 1992, A&A 259, L1
 Brunetti G., et al. 1999, in preparation
 Ensslin T.A., Lieu R., Biermann P.L., 1999, A&A in press; astro-ph/9808139
 Deiss B.M., Reich W., Lesch H., Wielebinski R., 1997, A&A 321, 55
 Feretti L., Dallacasa D., Giovannini G., Tagliani A., 1995, A&A 302, 680
 Fusco-Femiano R., Dal Fiume D., Feretti L., et al., 1999 ApJ 513, 197L
 Giovannini G., Feretti L., Venturi T., Kim K.T., Kronberg P.P., 1993, ApJ 406, 399
 Kim K.T., Kronberg P.P., Dewdney P.E., Landecker T.L., 1994, A&A 355, 29
 Hanisch R.J., Erickson W.C., 1980, AJ 85, 183
 Henning P., 1989, AJ 97, 1561
 Harris D.E., Grindlay J.E., 1979, MNRAS 188, 25
 Jaffe W.J., Perola G.C., 1973, A&A 26, 423
 Kardashev N.S., 1962, *Sov. Ast.* 6, 317
 Lieu R., Mittaz J.P.D., Bowyer S., et al., 1996, *Science* 274, 1335
 Rephaeli Y., Gruber D., Blanco P., 1999, ApJL 511, 21
 Sarazin C.L., 1999, ApJ in press; astro-ph/9901061
 Sarazin C.L., Lieu R., 1998, ApJL 494, 177
 Schlickeiser R., Sievers A., Thiemann H., 1987, A&A 182, 21
 Sreekumar P., Bertsch D.L., Dingus B.L., et al., 1996, ApJ 464, 628
 Venturi T., Giovannini G., Feretti L., 1990, AJ 99, 1381
 Völk H.J., Atoyan A.M., 1999, submitted to *Astropart. Physics*; astro-ph/9812458